Characterizing the Stability Region of IEEE 802.11 Distributed Coordination Function - Part I: Single Channel Analysis

Qingsi Wang and Mingyan Liu

Department of Electrical Engineering and Computer Science,

University of Michigan, Ann Arbor, MI 48109

Abstract

In this paper we model and characterize the stability region of IEEE 802.11 Distributed Coordination Function (DCF) both qualitatively and quantitatively. We also provide an intuitive explanation and verification by comparing it to the known stability region of slotted Aloha. We show that the size of backoff window plays a decisive role in shaping the corresponding stability region. Specifically, when the backoff window is sufficiently large, the stability region is convex, and it evolves into a concave region as the window size decreases. In addition, for given parameterization, there exists a unique stable region when the window size is sufficiently large, whereas smaller window sizes may lead to a collection of stability regions.

I. INTRODUCTION

As a widely deployed WLAN multiple access solution, the IEEE 802.11 Distributed Coordination Function (DCF) has been extensively studied, particularly in terms of its throughput performance. Such exercises provide insights in our understanding of the potential and limitation of 802.11 DCF. Generally speaking, the modeling of the throughput performance of 802.11 may be categorized into two classes, namely, one that focuses on the *saturated* regime and one on the *non-saturated* regime. Under the saturated case where each node is an infinite source, a mean field Markov model with great intuitive appeal was first proposed by Bianchi in his seminar work [1]. This model was shown to produce accurate prediction on the system throughput of a single *clique*, where all nodes interfere with each other. It has since motivated a large body of work on models of a similar nature, see e.g., [2] for a more general framework based on a simplified fixed point analysis using renewal theory. There has also been work studying the unsaturated case, which is often done by adding extra states to the original Markov chain proposed by Bianchi in [1], see e.g., [3], [4], [5]. In the unsaturated case the service processes across all nodes become coupled, thus characterizing the system throughput becomes much harder, and determining the queue stability region has been regarded as an open problem [6].

In this paper, we seek to characterize the *stability region* of 802.11 DCF for a clique of a finite number of users operating on a single channel. It is defined as the set of all arrival rates that can be stabilized by 802.11 DCF. We present a system of equations with feasibility constraints to describe this stability region. We then investigate the existence and uniqueness of its solutions. In particular, we show that there exists a unique solution to this system of equations when the size of the backoff window is sufficiently large. We further show that the size of the backoff window plays a decisive role in shaping the corresponding stability region. In particular, when the backoff window is sufficiently large, the corresponding stability region is convex; as the window size decreases it evolves into a concave region. We provide an intuitive explanation for this phenomenon, and connect this result to known results on slotted Aloha [7]. We note that while our discussion is focused on 802.11, our analytical framework is more generally applicable.

It is worth noting that results on the *rate* or *throughput capacity* region of 802.11 DCF are available in the literature [8], [9]. Technically, rate region and stability region are two different concepts: the former may be analyzed assuming all users are saturated while the latter by definition is a notion that is only applicable to a set of non-saturated users. In practice, studies have shown that in the case of slotted Aloha, its stability region is the same as the Shannon capacity region [7]. This might suggest that in the case of 802.11 DCF the two regions are also geometrically more similar than not. Results obtained in this paper seem to support this statement (more is discussed in Section IV), though fully validating it is out of the scope of the present paper and will be addressed in a future study.

The rest of this paper is organized as follows. In Section II we present our model and state definitions and assumptions. In Section III the aforementioned constrained system of equations termed $(\Sigma, C, \boldsymbol{\lambda})$ is presented to quantitatively describe the stability region, followed by an analysis on its solutions. Analytical results generated by the model are then compared to that from simulation in Section IV. We provide an intuitive explanation in Section V on the shape of the stability region by drawing results from slotted Aloha, and we conclude the paper in Section VI.

II. System Model and Preliminaries

Consider a multiple access system using the IEEE 802.11 DCF. We assume that

1) the system consists of n nodes (or users interchangeably), indexed by the set $\mathcal{N} = \{1, 2, \ldots, n\}$, each with an infinite buffer; each node uses the same parameterization and has one transceiver;

2) the channel is ideal and there is no MAC-level packet discard, i.e., there is no retransmission limit of a packet after collision;

3) the queueing process at each node is stationary and ergodic such that Little's law is applicable [10].

Throughout the analysis we will adopt occasional other simplifying assumptions to make the problem tractable; these are introduced in their respective specific context since some are applied locally and some globally in the modeling framework. These are summarized in Table II in the appendix. It should be noted that due to the complexity of the problem, successive simplification in the modeling effort is a rather common practice and has been used in most if not all previous works. We later show that these simplifications do not impact the accuracy of the model under normal operating parameter values.

The key to our method is to model the 802.11 DCF as a *slotted mean field Markov chain*. We first define the notion of a slot as follows.

Definition 1: Consider a virtual backoff timer of the system (or a virtual node) that counts down according to the 802.11 exponential backoff scheme with an infinite initial value. A *slot* is defined as the time interval between two successive decrements. Since the virtual node has no packet to send, it will alternate between the count down mode and the freezing mode indefinitely. The slot time is thus a random variable.

Remark 1: The above definition provides a universal slot time for all nodes in the system and we will assume that real backoff timers at a node is synchronized to this virtual timer on slot boundaries. The motivation behind such a construction originates from the principal difficulty in modeling a non-saturated system: the service process at each node runs in embedded time in terms of a slot, which is a random variable, whereas the packet arrival process is described in real-time [6]. This difficulty does not exist in saturated analysis, where arrival processes do not play a role.

Let the arrival rate at node i be λ_i bits per second, where $i \in \mathcal{N}$, and let $\boldsymbol{\lambda} = (\lambda_1, \lambda_2, \ldots, \lambda_n)$. We formally define the stability region of system as follows.

Definition 2: The *stability region* Λ is the set

$$\Lambda := \left\{ \boldsymbol{\lambda} \in \mathbb{R}_+^n \mid \text{queue lengths at all nodes are bounded with arrival rates } \boldsymbol{\lambda} \text{ under the 802.11 DCF scheme} \right\}.$$

For a given $\boldsymbol{\lambda}$, whether $\boldsymbol{\lambda} \in \Lambda$ is determined by the utilization factor at each node, denoted by ρ_i for node i, or equivalently the probability that the queue at node i is non-empty at an arbitrary real time instant. Let $\hat{\rho}_i$ be the probability that the queue at node i is non-empty at the beginning of an arbitrary slot, denoted by t^-. $\hat{\rho}_i$ is then given by

$$\hat{\rho}_i = P\big\{\text{the queue at node } i \text{ is non-empty at } t^-\big\}.$$

Note that $\hat{\rho}_i$ is conditioned on that t^- is the beginning of a slot, and thus $\hat{\rho}_i \neq \rho_i$ in general. Furthermore, we show in the appendix that $\hat{\rho}_i \leq \rho_i$ where equality holds if and only if $\rho_i = 1$ or $\rho_i = 0$, i.e., node i is either saturated or idle.

We next derive a relationship between transmission attempt probability and $\hat{\rho}_i$. Note that successive attempts by the same node may occur if a node repeatedly selects timer value 0 while other nodes freeze their timers. This phenomenon can be prominent when the window size is small. We will call the string of successive attempts a *run of attempts*, and the first attempt in a run a *run-first-attempt* or simply *first-attempt*. We will also use the term *backoff length* to mean the selected timer value plus 1.

A key assumption underlying our model is an *first-attempt collision sequence (FACS) decoupling approximation*, stated as follows. Define $C_i(j) := 1$ if the first-attempt of the jth run of attempts by node i results in a collision, and $C_i(j) := 0$ if it results in a success.

Assumption 1 (FACS Decoupling Approximation): For each node $i \in \mathcal{N}$, the first-attempt collision sequence $\{C_i(j)\}$ is i.i.d. with $P(C_i(j) = 1) = p_i$.

If one omits the possibility of successive attempts, or equivalently, assume that each run consists of only one attempt, which is reasonable when the initial window size is sufficiently large, then this decoupling approximation reduces to the well-known decoupling approximation by Bianchi [1].

Let τ_i be the probability that node i initiates a first-attempt in an arbitrary slot. Then, we have the following lemma.

Lemma 1: τ_i is given by $\tau_i = \hat{\rho}_i / \overline{W}_i$, where $\overline{W}_i$ is the average first-attempt backoff length of node i.

Proof: Define the following shorthand notations.

$$Tx := \big\{\text{node } i \text{ initiates a first-attempt in a slot}\big\};$$
$$Q(\overline{Q}) := \big\{\text{the queue at node } i \text{ is non-empty (empty) at the beginning of a slot}\big\}.$$

We then have

$$\tau_i = P(Tx|Q) \cdot P(Q) + P(Tx|\overline{Q}) \cdot P(\overline{Q}).$$

Since $P(Tx|Q) = \frac{1}{\overline{W}_i}$, $P(Tx|\overline{Q}) = 0$, the result follows.[1] ■

Remark 2: If the possibility of runs of attempts is neglected, i.e., FACS decoupling reduces to Bianchi's approximation, then $\overline{W}_i$ is given by

$$\overline{W}_i = \frac{1}{2}\left[W\left((1-p_i)\sum_{j=0}^{m-1}(2p_i)^j + (2p_i)^m \right) + 1 \right], \tag{1}$$

where W is the size of the initial backoff window and m is the value of the maximum backoff stage. Furthermore, if we consider the saturated case where users are identical, we have $\hat{\rho}_i = \rho_i = \rho = 1$, and $p_i = p$, for all i. Consequently,

$$\tau_i = \tau = \frac{2}{W\left((1-p)\sum_{j=0}^{m-1}(2p)^j + (2p)^m \right) + 1}$$

$$= \frac{2(1-2p)}{(1-2p)(W+1) + pW(1-(2p)^m)},$$

which is the same result obtained in [1].

We conclude this section by noting that not all our assumptions are applied globally, e.g., successive attempts are ignored when computing the average first-attempt backoff length and $\overline{W}_i$ is hence given by Eqn. (1), but successive attempts are critically considered when computing the average length of a slot given various conditions. These are summarized in Table II.

III. SINGLE CHANNEL ANALYSIS

A. The stability region equation Σ

Our first main result is the following theorem on the quantitative description of Λ.

Theorem 1: $\boldsymbol{\lambda} \in \Lambda$ if and only if there exists at least one solution $\boldsymbol{\tau} = (\tau_1, \tau_2, \ldots, \tau_n)$ to the following constrained system of equations $(\Sigma, \mathrm{C}, \boldsymbol{\lambda})$,

$$\Sigma : \begin{cases} \tau_i = \dfrac{\hat{\rho}_i}{\overline{W}_i} & \text{(a)} \\[2mm] p_i = 1 - \displaystyle\prod_{j \neq i}(1 - \tau_j) & \text{(b)} \\[2mm] \rho_i = \min\left\{ \dfrac{\lambda_i}{P}\left(\dfrac{\overline{W}_i - 1}{1 - p_i}\mathbb{E}[slot_{i,Q,\overline{Tx}}] + T_c\dfrac{p_i}{1 - p_i} + T_s \right), 1 \right\} & \text{(c)} \end{cases}$$

subject to

$$\mathrm{C} : \begin{cases} 0 \leq \tau_i \leq 1 & \text{(i)} \\ 0 \leq \rho_i < 1 & \text{(ii)} \end{cases}$$

for all $i \in \mathcal{N}$. Here P is the packet payload size; $\mathbb{E}[slot_{i,Q,\overline{Tx}}]$ is the conditional average length of a slot given that the queue at node i is non-empty but i does not transmit in this slot; T_s and T_c are the lengths of a successful transmission and a collision, respectively.

Proof: Σ(a) is the result of Lemma 1, and Σ(b) is an immediate consequence of its definition. Let the average packet service time at node i be $\overline{X}_i^p$ seconds per packet. Therefore,

$$\overline{X}_i^p = \sum_{j=1}^{\infty}\left[(p_i)^j\left(T_c + \left(\frac{2^{\min\{j,m\}}W + 1}{2} - 1 \right) \times \mathbb{E}[slot_{i,Q,\overline{Tx}}] \right) \right] + \left(\frac{W+1}{2} - 1 \right)\mathbb{E}[slot_{i,Q,\overline{Tx}}] + T_s$$

$$= \sum_{j=0}^{\infty}\left[\frac{2^{\min\{j,m\}}W - 1}{2}(p_i)^j \right]\mathbb{E}[slot_{i,Q,\overline{Tx}}] + T_c\sum_{j=1}^{\infty}(p_i)^j + T_s$$

$$= \frac{\overline{W}_i - 1}{1 - p_i}\mathbb{E}[slot_{i,Q,\overline{Tx}}] + T_c\frac{p_i}{1 - p_i} + T_s.$$

Note that we have suppressed successive attempts in the above. The average data service time is $\overline{X}_i = \overline{X}_i^p/P$. Thus, by Little's Law, the utilization factor of node i is given by $\rho_i = \min\{\lambda_i\overline{X}_i, 1\}$ and Σ(c) follows. C(i) is for the validity of τ as a probability measure. $(\Sigma, \mathrm{C}(i), \boldsymbol{\lambda})$ then constitutes a full set of description on the system utilization. C(ii) is the necessary and sufficient condition for a stable queueing system. ■

---

[1]Technically the first equality is an approximation; similar approximations have been adopted in related work like [11].

For a given set of system parameter values, two sets of quantities are needed to compute Σ: $\mathbb{E}[slot_{i,Q,\overline{Tx}}]$ and $\hat{\rho}_i$, $\forall i \in \mathcal{N}$. These are computed in Appendix B and C, respectively. In particular, in Appendix C we show that though it is analytically intractable, $\hat{\rho}_i$ is well approximated by

$$\hat{\rho}_i \approx \frac{\rho_i \mathbb{E}[slot_{i,\overline{Q}}]}{\rho_i \mathbb{E}[slot_{i,\overline{Q}}] + (1 - \rho_i)\mathbb{E}[slot_{i,Q}]},$$

where $\mathbb{E}[slot_{i,Q}]$ ($\mathbb{E}[slot_{i,\overline{Q}}]$) is the conditional average length of a slot, given that the queue at node i is non-empty (resp. empty) at the beginning of this slot.

B. Characteristics of solutions to Σ

Without the stability constraint C(ii), (Σ, C(i), $\boldsymbol{\lambda}$) can be rewritten as a vector equation in $[0,1]^n$, that is,

$$\boldsymbol{\tau} = \boldsymbol{\Gamma}(\boldsymbol{\tau}),$$

where $\boldsymbol{\tau} = (\tau_1, \tau_2, \ldots, \tau_n) \in [0,1]^n$, and the existence of solutions can be then shown by Brouwer's fixed point theorem. However, the uniqueness of solution is in general difficult to prove; nevertheless, under the condition of a sufficiently large initial backoff window W, we have the following result on the uniqueness of solution.

Theorem 2: For sufficiently large W, $(\Sigma, \boldsymbol{\lambda})$ admits a unique solution.

Proof: See Appendix D. ∎

Remark 3: 1) Note that in the above theorem the condition is on the initial window size W. As an approximation we will take this to be equivalent to a large average backoff window assumption. This is because the probability of a (first-attempt) collision decays inverse-linearly in W, and thus $\overline{W}_i$ is dominated by W when W is sufficiently large.

2) As we will see in the next section, multiple fixed point solutions may arise when W is small; this will be referred to as multi-equilibria (as opposed to "multistable" or "metastable" [6] to avoid confusion).

In the proof of Theorem 2, we in fact obtained the approximated unique solution to $(\Sigma, \boldsymbol{\lambda})$. Therefore, by imposing feasibility constraints C, we can induce a simplified version of $(\Sigma, C, \boldsymbol{\lambda})$ which is equivalently an approximation of Λ. The above observation is summarized in the following corollary.

Corollary 1: When W is sufficiently large, Λ is approximated by

$$\tilde{\Lambda} = \left\{ \boldsymbol{\lambda} \in \mathbb{R}_+^n \;\middle|\; 0 < \frac{\gamma_i^1(\lambda_i) \sum_j \gamma_j^2(\lambda_i)}{1 - \sum_i \gamma_j^1(\lambda_i)} + \gamma_i^2(\lambda_i) < \frac{2}{W+1}, \forall i \in \mathcal{N} \right\},$$

where

$$\gamma_i^1(\lambda_i) = \frac{\lambda_i T}{P} \Big/ \left(1 + \frac{\lambda_i T}{P}\right),$$

and

$$\gamma_i^2(\lambda_i) = \left(\frac{\lambda_i T}{P} - \frac{\lambda_i(W-1)(T-\sigma)}{P(W+1)}\right) \Big/ \left(1 + \frac{\lambda_i T}{P}\right).$$

Within the context of a unique solution to $(\Sigma, C, \boldsymbol{\lambda})$, consider $\boldsymbol{\lambda}$ as input parameters and rewrite Σ as $\mathbf{F}(\boldsymbol{\tau}, \boldsymbol{\lambda}) = 0$, with $(n+n)$ unknowns, i.e., τ_i's and λ_i's. We can then inspect the existence of an implicit function of $\boldsymbol{\tau}$ in terms of $\boldsymbol{\lambda}$, and for this we need to examine the invertibility of the corresponding Jacobian matrix. Note also that the correspondence between ρ_i and $(\boldsymbol{\lambda}, \boldsymbol{\tau})$ given by $\Sigma(c)$ is a continuous function. If the Jacobian is invertible on the boundary of the stability region Λ in the space $\mathbb{R}_+^n$, then the continuity of $\rho_i = \rho_i(\boldsymbol{\lambda})$ is established. Hence, on the boundary of Λ, denoted by $\partial\Lambda$, there exists at least one node i such that $\rho_i = 1$. However, to determine the invertibility of the Jacobian on $\partial\Lambda$ is highly non-trivial and in general analytically intractable when the number of nodes is large. Therefore, we have resorted to numerical evaluation and more is discussed in the next section.

IV. NUMERICAL RESULTS

In this section we present numerical results obtained from a numerical solver and simulation that we implemented on MATLAB 2008b platform. Specifically, we consider a system of two users. We reconstruct Σ as a fixed point equation in the form $(\boldsymbol{\tau}, \hat{\boldsymbol{\rho}}) = \boldsymbol{\Gamma}'(\boldsymbol{\tau}, \hat{\boldsymbol{\rho}})$ in the solver, where $\boldsymbol{\tau} = (\tau_i, i \in \mathcal{N})$ and $\hat{\boldsymbol{\rho}} = (\hat{\rho}_i, i \in \mathcal{N})$, and it is solved with an iterative procedure. Solving for $(\boldsymbol{\tau}, \hat{\boldsymbol{\rho}})$ simultaneously rather than $(\boldsymbol{\tau}, \boldsymbol{\rho})$ or simply $\boldsymbol{\tau}$ is a choice that makes this model easier to solve in the case of a multi-channel system, which is reported in [12]. The parameters used in both the solver and the simulation are reported in Table III in the appendix. We consider the basic access mechanism of DCF in this paper, and have

$$\begin{cases} T_s = \frac{P}{\text{Tx. Rate}} + \text{Header} + \text{ACK} + \text{DIFS} + \text{SIFS} + 2\delta \\ T_c = \frac{P}{\text{Tx. Rate}} + \text{Header} + \text{DIFS} + \delta \end{cases}$$

where δ is the propagation delay.
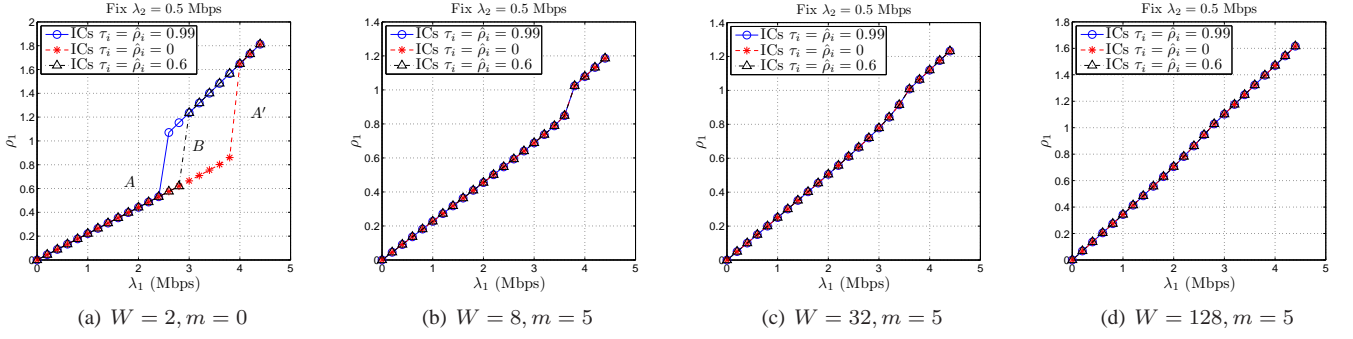
Fig. 1. Solution components for various scenarios: an illustration.
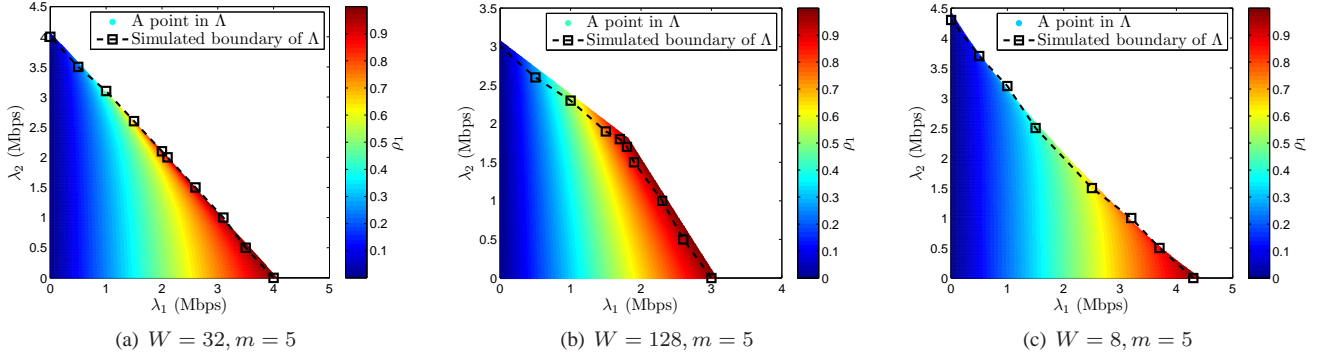
Fig. 2. The stability regions in various scenarios - part I.
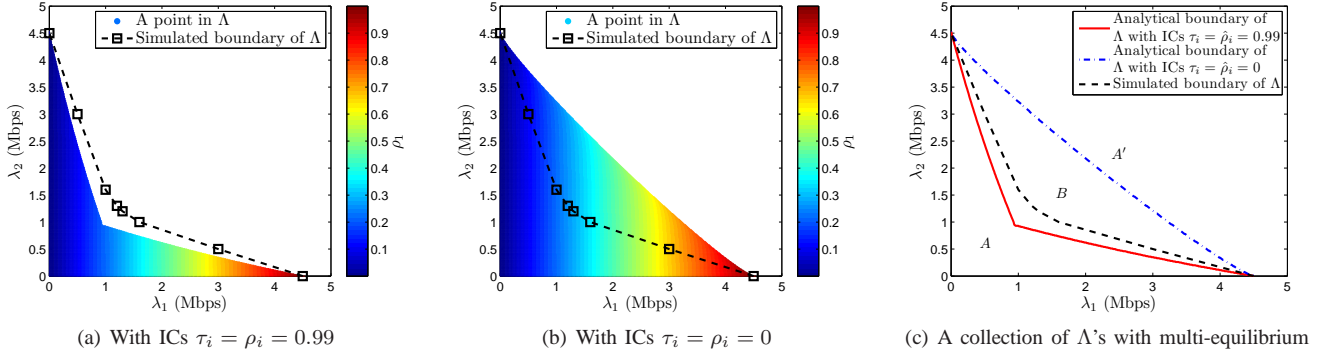
Fig. 3. The stability regions in various scenarios - part II: $W = 2$ and $m = 0$.
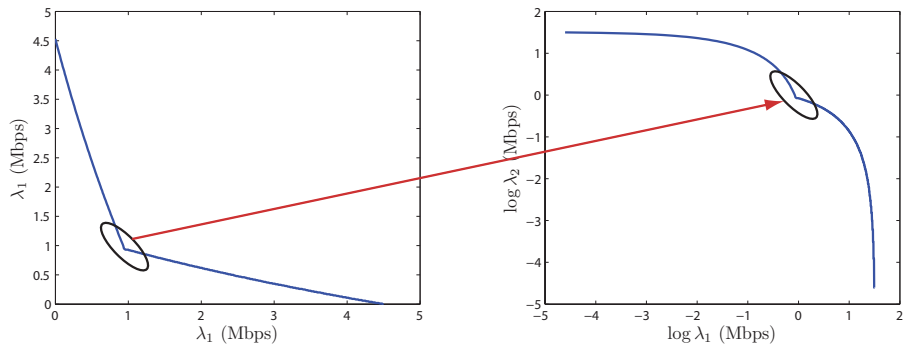
Fig. 4. The lower contour of Λ when $W = 2$ and $m = 0$ in the logarithmic scale.

A. Multi-equilibrium and discontinuity in ρ

We first illustrate the existence of multi-equilibrium solutions and discontinuity of $\rho_i(\boldsymbol{\lambda})$ with respect to $\boldsymbol{\lambda}$; this is shown in Figure 1. We fix the value of λ_2 and increase λ_1 from 0 to 4.5 Mbps. For each pair $\boldsymbol{\lambda} = (\lambda_1, \lambda_2)$, we solve the fixed point(s) of $\boldsymbol{\Gamma}'$ with the same set of initial values of τ_i and $\hat{\rho}_i$ for $i \in \mathcal{N}$ to which we later refer as a set of initial conditions (ICs), and we convert the results to $\boldsymbol{\rho} = (\rho_i, i \in \mathcal{N})$ accordingly. The collection of the pairs $(\boldsymbol{\lambda}, \boldsymbol{\rho}(\boldsymbol{\lambda}))$ then forms a *solution component* for this set of ICs. Notice that this is obtained by solving $(\Sigma, \text{C(i)}, \boldsymbol{\lambda})$ without considering the stability constraint C(ii). We repeat the above computation for different sets of ICs under the same system parameters including W and m. The entire process is then repeated for different pairs (W, m). For each pair (W, m), the resulting solution components constitute an overall correspondence between the vectors $\boldsymbol{\lambda}$ and $\boldsymbol{\rho}(\boldsymbol{\lambda})$, and this is plotted as ρ_1 vs. λ_1 in Figure 1.

In the first scenario as shown in Figure 1(a), where the initial window is of the smallest possible size for two users and window expansion is disallowed ($m = 0$), three different zones of the correspondence $\rho_1(\lambda_1)$ are present, labeled as A, A' and B in the figure. In zones A and A', single fixed point is admitted and $\rho_1(\lambda_1)$ reduces to a function, while in zone B we see two solutions. Along each solution component, there is a jump in ρ_1 in zone B as λ_1 increases; this is essentially a phase transition from stable to unstable. What this result illustrates is that depending on the initial condition, certain input rates may or may lead to a feasible solution (a point in the stability region). Thus when such multi-equilibrium exists, we may have a collection of stability region Λ's.

Intuitively, ICs with large values suggest a pessimistic prediction on the system stability under $\boldsymbol{\lambda}$, and it may thus result in a small Λ; by contrast, ICs with small values render an optimistic one and a larger Λ. Empirically, we find that the set of ICs with $\tau_i = \rho_i \approx 1$ for $i \in \mathcal{N}$ results in the earliest jump in ρ_1 and the one with $\tau_i = \rho_i = 0$ for $i \in \mathcal{N}$ gives the latest. Consequently, solution components resulting from these two sets of ICs define the boundary of zone B and the corresponding stability regions, forming the supremum and infimum of the collection of Λ's.

Inspecting the set of figures Fig. 1(a)-1(d), we see that as the initial window increases, the multi-equilibrium gradually vanishes and the gap in ρ_1 caused by the jump discontinuity closes.

B. Numerical and empirical stability regions

We numerically solve $(\Sigma, \text{C}, \boldsymbol{\lambda})$ with two nodes to obtain the corresponding Λ, and then compare with the simulated boundary. In simulation, for each fixed λ_2, we increase λ_1 with a step size $\Delta\lambda$. Denote by $S^{\boldsymbol{\lambda}}$ the empirical throughput obtained under $\boldsymbol{\lambda}$, by $B^{\boldsymbol{\lambda}}$ the total number of backlogged packets in the system, and by T_f the total simulated time. The simulator declares a point $\boldsymbol{\lambda}$ to be unstable if $S^{\boldsymbol{\lambda}} < \lambda_1 + \lambda_2$ and $B^{\boldsymbol{\lambda}}P > \alpha \cdot (\lambda_1 + \lambda_2)T_f$, where α is an instability threshold and $0 < \alpha < 1$. In our experiment, we set $\Delta\lambda = 0.1$Mbps (100 Kbps), $T_f = 10$s and $\alpha = 1\%$. The stable point (λ_1, λ_2) such that $(\lambda_1 + \Delta\lambda, \lambda_2)$ is unstable is recorded as a point on the simulated boundary. The results are shown in Figure 2. Also, all the stability regions are scaled accordingly with respect to the length of a slot in real time units.

Our main observation is that when the initial (or average) backoff window is large, the stability region is convex (Figure 2(b)). The convexity gradually disappears as the window size decreases and the region is given by a near-linear boundary in Figure 2(a). It becomes clearly concave when the window size is small (Figure 2(c)). Interestingly, the case of $W = 32$ is the most often studied in the literature, and the linear boundary of the capacity region has been observed in [8]. As shown here, this linear boundary is only a special case in a spectrum of convex-concave boundaries. In [9], Leith *et al.* established the general log-convexity of the rate region of 802.11 WLANs. In Figure 4, we numerically show that the stability region obtained above is also log-convex, except the bump caused by the nondifferentiable point due to the numerical instability of solver under the extreme parameterization. Therefore, our results support the belief that the rate region and the stability region are quite similar in feature. This however is not a formally proven statement, nor are we aware of such in the case of 802.11.

The change in the shape of the stability region as W changes may be explained as follows. Small W represents a highly aggressive configuration. This is much more beneficial when there is a high degree of asymmetry between the users' arrival rates. This is reflected in the concave shape of the region. When W is large, users are non-aggressive, which is more beneficial when arrival rates are similar, resulting in the convex shape. Numerically, the $W = 8$ case gives the largest stability region. This seems to suggest that the largest stability region is given by the smallest choice of W such that a unique feasible solution to $(\Sigma, \text{C}, \boldsymbol{\lambda})$ exists. It would be very interesting to see if this could be established rigorously.

In Figure 3, we compute the stability regions of the case where $W = 2$ and $m = 0$ for two different sets of ICs. As discussed earlier in this section, when multi-equilibrium exists we may have a collection of stability regions. This is clearly seen in Figure 3: three different zones A, A' and B in the correspondence $\rho_1(\lambda_1)$ are mapped accordingly onto Λ. From these results, we may interpret that in zones A (A'), the system is uniformly stable (resp. unstable) regardless of the ICs, while in zone B the stability of system depends on the ICs. As summarized in [6], the simulated observation reflects time-averages of multiple equilibria.

C. Approximation of Λ

In Corollary 1, we obtained a simplified version of $(\Sigma, \text{C}, \boldsymbol{\lambda})$ which can be computed with significantly reduced complexity and provides $\tilde{\Lambda}$, an approximation of Λ. We are then interested in how accurate this approximation can be, and numerical

results are reported in Figure 5. Roughly summarizing, as the backoff window enlarges, $\tilde{\Lambda}$ approaches Λ, and the main source of loss of accuracy roots in the approximation $\hat{\rho}_i = \rho_i$ which results in a gap between the boundaries of $\tilde{\Lambda}$ and Λ. Nonetheless, we are still unable to obtain a more close approximation of $\hat{\rho}_i$ reducing Σ to a computationally friendly form as given in Corollary 1, and we leave it as one potential topic to investigate in our future work.

(a) $W = 32, m = 5$ (b) $W = 64, m = 5$ (c) $W = 128, m = 5$
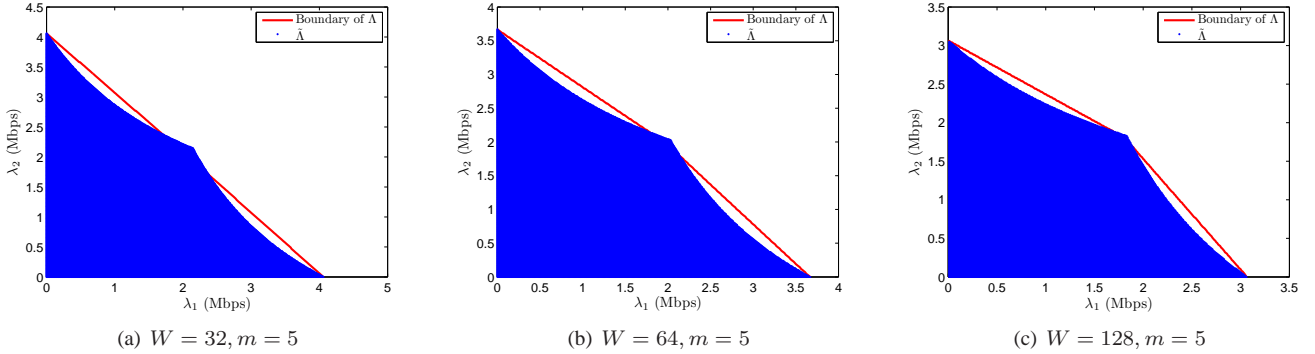
Fig. 5.   Approximated stability region.

V. FROM 802.11 DCF BACK TO ALOHA

The slotted Aloha protocol is the natural prototype of the modern IEEE 802.11 DCF scheme. In this section, we first recall results on the stability region of slotted Aloha, and then provide an intuitive argument on why the qualitative properties of the stability region of 802.11 DCF shown in the previous section are to be expected.

In [13], Massey and Mathys studied an information theoretical model of multiaccess channel which shares several fundamental features with slotted Aloha. They investigated the Shannon capacity region of this channel with n users, which is shown to be the following subset of $\mathbb{R}^n_+$,

$$C = \left\{ \text{vect}\left(p_i \prod_{j \neq i}(1 - p_j) \right) \ \middle|\ 0 \leq p_i \leq 1, 1 \leq i \leq n \right\},$$

where $\text{vect}(v_i) = (v_1, v_2, \ldots, v_n)$, and p_i can be interpreted as the transmission attempt rate of user i. In [7], Anantharam showed that the closure of the stability region of slotted Aloha is also given by C, under a geometrically distributed aggregate arrival process with parameter $1/(\sum_i \lambda_i)$ and with the probability that such an arrival is at node i being $\lambda_i / \sum_j \lambda_j$.
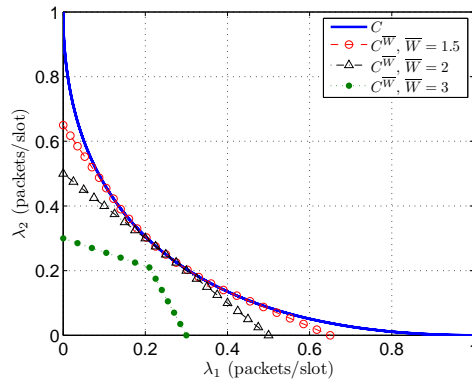
Fig. 6.   The stability region of slotted ALOHA and induced subsets.

The above result on slotted Aloha can be used to explain the stability region of 802.11 DCF. Note that the main difference between the two lies in the collision avoidance mechanism. Instead of attempting transmission with probability $0 \leq p \leq 1$ in a slot under slotted Aloha, in 802.11 each user adopts a backoff process with a randomly chosen timer value (or backoff length) within a window of size W. The effect the average length $\overline{W}$ has on transmission under 802.11 is akin to that of restricting the attempt rate p within an upper bound $\frac{1}{\overline{W}}$ under slotted Aloha. Hence, the stability region of 802.11 DCF may be thought of as a subset of C provided that we properly scale a slot to real time.

To verify this intuition, let $C^{\overline{W}}$ be the subset of C when $0 \leq p_i \leq \frac{1}{\overline{W}}$ for all i. In Figure 6, we plot C and $C^{\overline{W}}$ with different values of $\overline{W}$. As can be seen, as $\overline{W}$ grows, $C^{\overline{W}}$ evolves from a concave set to a convex set, consistent with what we

observed of 802.11 DCF in the previous section. It must be pointed out that the connection described above, while intuitive, is not a precise one technically. For instance, this connection might suggest that the stability region of 802.11 DCF will reduce to C when the average backoff length is 1. This is however not true. In this trivial case, the stability region of 802.11 DCF is reduced to one dimensional, i.e., the system is unstable for $n \geq 2$. This is because the retransmission probability of 802.11 is also lower bounded by the reciprocal of window size at its backoff stage, and in the case when the backoff length (or window) is one another collision surely occurs.

VI. Concluding Remarks

In this paper, we identified the stability region of 802.11 DCF. An interesting finding is that as the window size W increases, the stability region changes from concave to convex. In addition, this region is unique when W is sufficiently large, whereas it depends on the initial condition of the system when W is small due to multi-equilibrium solutions to a system of equations. Our ongoing research aims at extending this result to a multi-channel system, and preliminary results in this direction are presented in [12].

Appendix A
Proof of $\hat{\rho}_i \leq \rho_i$

We first define the following stochastic processes generated by the queueing process at node i.

$T_{i,Q}(t) :=$ the total length of real time periods that the queue at node i is non-empty (or i is busy) up to time t;

$T_{i,\overline{Q}}(t) :=$ the total length of real time periods that the queue at node i is empty (or i is idle) up to time t;

$N_{i,Q}(t) :=$ the total number of slots that the queue at node i is non-empty at its beginning up to time t;

$N_{i,\overline{Q}}(t) :=$ the total number of slots that the queue at node i is empty at its beginning up to time t.

These processes are well-defined on the same space Ω, and then because of the ergodicity assumption, ρ_i and $\hat{\rho}_i$ can be expressed alternatively as

$$\rho_i = \lim_{t \to \infty} \frac{T_{i,Q}(\omega, t)}{t} = \lim_{t \to \infty} \frac{T_{i,Q}(\omega, t)}{T_{i,Q}(\omega, t) + T_{i,\overline{Q}}(\omega, t)},$$

and

$$\hat{\rho}_i = \lim_{t \to \infty} \frac{N_{i,Q}(\omega, t)}{N_{i,Q}(\omega, t) + N_{i,\overline{Q}}(\omega, t)},$$

for all $\omega \in \Omega$. Let $\Delta_i(t)$ be the total time fragmentation of busy periods in idle slots of node i up to time t, and let $S_{i,Q}(k)$ ($S_{i,\overline{Q}}(k)$) be the length of kth busy (resp. idle) slot. Quantities described above are illustrated in Figure 7. Then, we have

$$T_{i,Q}(t) - \Delta_i(t) = \sum_{k=1}^{N_{i,Q}(t)} S_{i,Q}(k),$$

and

$$t = \sum_{k=1}^{N_{i,Q}(t)} S_{i,Q}(k) + \sum_{k=1}^{N_{i,\overline{Q}}(t)} S_{i,\overline{Q}}(k).$$

Therefore,

$$\rho_i \geq \lim_{t \to \infty} \frac{T_{i,Q}(\omega, t) - \Delta_i(\omega, t)}{t}$$

$$= \lim_{t \to \infty} \frac{\sum_{k=1}^{N_{i,Q}(\omega, t)} S_{i,Q}(\omega, k)}{\sum_{k=1}^{N_{i,Q}(\omega, t)} S_{i,Q}(\omega, k) + \sum_{k=1}^{N_{i,\overline{Q}}(\omega, t)} S_{i,\overline{Q}}(\omega, k)}$$

$$= \lim_{t \to \infty} \left[\frac{\sum_{k=1}^{N_{i,Q}(\omega, t)} S_{i,Q}(\omega, k)}{N_{i,Q}(\omega, t)} N_{i,Q}(\omega, t) \middle/ \left(\frac{\sum_{k=1}^{N_{i,Q}(\omega, t)} S_{i,Q}(\omega, k)}{N_{i,Q}(\omega, t)} N_{i,Q}(\omega, t) + \frac{\sum_{k=1}^{N_{i,\overline{Q}}(\omega, t)} S_{i,\overline{Q}}(\omega, k)}{N_{i,\overline{Q}}(\omega, t)} N_{i,\overline{Q}}(\omega, t) \right) \right].$$

Let $\mathbb{E}[slot_{i,Q}]$ and $\mathbb{E}[slot_{i,\overline{Q}}]$ be the conditional average lengths of an arbitrary slot, given that the queue at node i is non-empty or empty at the beginning of slot, respectively. We claim that $\mathbb{E}[slot_{i,Q}] > \mathbb{E}[slot_{i,\overline{Q}}]$, and $N_{i,Q}(t) \to \infty$ and $N_{i,\overline{Q}}(t) \to \infty$ as $t \to \infty$. Consequently, following the ergodicity, we obtain

$$\rho_i \geq \lim_{t \to \infty} \frac{N_{i,Q}(\omega, t)\mathbb{E}[slot_{i,Q}]}{N_{i,Q}(\omega, t)\mathbb{E}[slot_{i,Q}] + N_{i,\overline{Q}}(\omega, t)\mathbb{E}[slot_{i,\overline{Q}}]}$$
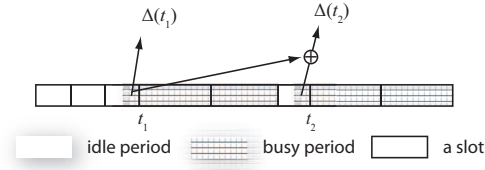
Fig. 7.   Slotted time dynamics.

$$\geq \lim_{t \to \infty} \frac{N_{i,Q}(\omega, t)}{N_{i,Q}(\omega, t) + N_{i,\overline{Q}}(\omega, t)}$$

$$= \hat{\rho}_i.$$

It remains to justify the claims made above, and they appear in Appendix B.

APPENDIX B
COMPUTATION OF $\mathbb{E}[slot_{\{\cdot\}}]$ AND RELATED QUANTITIES

Given an event $\{\cdot\}$, let $P_{idle;\{\cdot\}}$, $P_{succ;\{\cdot\}}$ and $P_{coll;\{\cdot\}}$ be the conditional probabilities that this slot is idle, that the first-attempt in the slot is a success, and that the first-attempt is a collision, respectively. Notice that $P_{coll;\{\cdot\}} = 1 - P_{idle;\{\cdot\}} - P_{succ;\{\cdot\}}$. Also, denote by $L_{idle;\{\cdot\}}$, $L_{succ;\{\cdot\}}$ and $L_{coll;\{\cdot\}}$ the average lengths of the slot in the corresponding cases. Let $\mathbb{E}[slot_{\{\cdot\}}]$ be the conditional average length of a slot. Therefore,

$$\mathbb{E}[slot_{\{\cdot\}}] = \sum_{s \in \{idle, succ, coll\}} P_{s;\{\cdot\}} \cdot L_{s;\{\cdot\}}.$$

As for $L_{s;\{\cdot\}}$, where $s \in \{idle, succ, coll\}$, we have

$$L_{idle;\{\cdot\}} = \sigma,$$

$$L_{succ;\{\cdot\}} = T_s \sum_{i=0}^{\infty} \left(\frac{1}{W}\right)^i = \frac{1}{1 - \frac{1}{W}} T_s,$$

and

$$L_{coll;\{\cdot\}} \approx T_c + \sum_{i=1}^{\infty} \left\{ \left[\left(\frac{1}{\overline{CW}_{\{\cdot\}}}\right)^2\right]^i T_c + \left[\left(\frac{1}{\overline{CW}_{\{\cdot\}}}\right)^2\right]^{i-1} \times \frac{1}{\overline{CW}_{\{\cdot\}}} \left(1 - \frac{1}{\overline{CW}_{\{\cdot\}}}\right) \frac{1}{1 - \frac{1}{W}} T_s \right\}$$

$$= \frac{1}{1 - \left(\frac{1}{\overline{CW}_{\{\cdot\}}}\right)^2} T_c + \frac{1}{\left(1 + \overline{CW}_{\{\cdot\}}\right)\left(1 - \frac{1}{W}\right)} T_s$$

$$\approx \frac{1}{1 - \left(\frac{1}{W}\right)^2} T_c + \frac{1}{W - \frac{1}{W}} T_s,$$

where σ, T_s and T_c are the lengths of an empty system slot, a successful transmission, and a collision, respectively; $\overline{CW}_{\{\cdot\}}$ is the conditional average backoff window size. These quantities are well-defined when $W \geq 2$ which is presumed in application. The first approximation of $L_{coll;\{\cdot\}}$ is due to omitting the possibility of collisions involving three or more nodes, and the other one results from substituting $\overline{CW}_{\{\cdot\}}$ with the initial backoff window size W. Note that, if we neglect successive attempts, we have $L_{succ;\{\cdot\}} = T_s$ and $L_{coll;\{\cdot\}} = T_c$, which is also a natural consequence when W is sufficiently large in the above equations. Define then by $\tau_{i,Q}$ the conditional probability that node i transmits in an arbitrary slot, given its queue is non-empty at the beginning of this slot, and hence we have $\tau_{i,Q} = \frac{1}{W_i}$. Consequently,

$$P_{idle;i,\overline{Q}} = \prod_{j \neq i} (1 - \tau_j),$$

$$P_{succ;i,\overline{Q}} = \sum_{j \neq i} \tau_j \prod_{l \neq i,j} (1 - \tau_l),$$

$$P_{idle;i,Q} = (1 - \tau_{i,Q}) \prod_{j \neq i} (1 - \tau_j),$$

$$P_{succ;i,Q} = \sum_l t_l \prod_{j \neq l} (1 - t_l),$$

where

$$t_j = \begin{cases} \tau_{i,Q}, & \text{if } j = i \\ \tau_j, & \text{if } j \neq i \end{cases}.$$

Since $P_{idle;i,Q} < P_{idle;i,\overline{Q}}$ and $\sigma < T_s, T_c$, we have $\mathbb{E}[slot_{i,Q}] > \mathbb{E}[slot_{i,\overline{Q}}]$. In addition, it is clear that $\mathbb{E}[slot_{\{.\}}]$ is finite, and thus $N_{i,Q}(t) \to \infty$ and $N_{i,\overline{Q}}(t) \to \infty$ as $t \to \infty$ when $0 < \rho_i < 1$. Explicit expressions for other varieties of $\mathbb{E}[slot_{\{.\}}]$ that are used throughout the paper are reported in Table I.

APPENDIX C
APPROXIMATION OF $\hat{\rho}_i$

Due to the analytical intractability of $\Delta_i(t)$, we are interested in proper approximations of $\hat{\rho}_i$, thus resulting in good estimation of Λ, where the goodness in the context of our stability study is regarded as a tight underestimation. Recalling that $\hat{\rho}_i \leq \rho_i$ and equality holds if and only if $\rho_i = 1$ or $\rho_i = 0$, therefore by replacing $\hat{\rho}_i$ by ρ_i in Σ(c), solutions to the resulting system of equations form an underestimation of Λ but accurate when $\rho_i = 1$ or 0 for all i. Moreover, by noticing that

$$\hat{\rho}_i = \lim_{t \to \infty} \frac{\frac{T_{i,Q}(\omega,t) - \Delta_i(\omega,t)}{\mathbb{E}[slot_{i,Q}]}}{\frac{T_{i,Q}(\omega,t) - \Delta_i(\omega,t)}{\mathbb{E}[slot_{i,Q}]} + \frac{T_{i,\overline{Q}}(\omega,t) + \Delta_i(\omega,t)}{\mathbb{E}[slot_{i,\overline{Q}}]}}$$

$$\leq \lim_{t \to \infty} \frac{T_{i,Q}(\omega,t)\mathbb{E}[slot_{i,\overline{Q}}]}{T_{i,Q}(\omega,t)\mathbb{E}[slot_{i,\overline{Q}}] + T_{i,\overline{Q}}(\omega,t)\mathbb{E}[slot_{i,Q}]}$$

$$\leq \rho_i,$$

and defining

$$\hat{\hat{\rho}}_i = \lim_{t \to \infty} \frac{T_{i,Q}(\omega,t)\mathbb{E}[slot_{i,\overline{Q}}]}{T_{i,Q}(\omega,t)\mathbb{E}[slot_{i,\overline{Q}}] + T_{i,\overline{Q}}(\omega,t)\mathbb{E}[slot_{i,Q}]}$$

$$= \frac{\rho_i\mathbb{E}[slot_{i,\overline{Q}}]}{\rho_i\mathbb{E}[slot_{i,\overline{Q}}] + (1 - \rho_i)\mathbb{E}[slot_{i,Q}]},$$

we have $\hat{\rho}_i \leq \hat{\hat{\rho}}_i \leq \rho_i$. Hence, substituting $\hat{\rho}_i$ with $\hat{\hat{\rho}}_i$ in Σ(c), we can obtain a tighter underestimation of the Λ, trading off with higher computational complexity compared to the previous approximation. Empirical results suggest that $\hat{\hat{\rho}}$ is sufficiently close to $\hat{\rho}$, and we use $\hat{\hat{\rho}}$ as $\hat{\rho}$ throughout our computation.

APPENDIX D
PROOF OF THEOREM 2

First of all, with a large backoff window, the probability of collision is small, so we have $\overline{W}_i \approx \frac{W+1}{2}$. We also observe that $\mathbb{E}[slot_{i,Q}] \approx \mathbb{E}[slot_{i,\overline{Q}}]$ since $\tau_{i,Q} = \frac{1}{\overline{W}_i}$ and W is large. Consequently,

$$\hat{\rho}_i \approx \frac{\rho_i\mathbb{E}[slot_{i,\overline{Q}}]}{\rho_i\mathbb{E}[slot_{i,\overline{Q}}] + (1 - \rho_i)\mathbb{E}[slot_{i,Q}]} \approx \rho_i.$$

Let $T_s = T_c = T$ for the simplicity of presentation. Then, Σ is approximated by the following system of equations,

$$\widetilde{\Sigma} : \begin{cases} \tau_i = \dfrac{\rho_i}{\frac{W+1}{2}} & \text{(a)} \\[3mm] p_i = 1 - \displaystyle\prod_{j \neq i}(1 - \tau_j) & \text{(b)} \\[3mm] \rho_i = \dfrac{\lambda_i}{P}\left[\dfrac{\frac{W+1}{2} - 1}{1 - p_i}\left(\sigma\displaystyle\prod_{j \neq i}(1 - \tau_j) + T\left(1 - \displaystyle\prod_{j \neq i}(1 - \tau_j)\right)\right) + T\dfrac{p_i}{1 - p_i} + T\right] & \text{(c)} \end{cases}$$

Note that with the constraint of C(ii), the explicit unit upper-bound on ρ_i is not necessary, and thus we can suppress this upper-bound in Σ(c). Substituting $\widetilde{\Sigma}$(b) and (c) in (a), we obtain

$$\tau_i = \frac{2\lambda_i}{P(W+1)}\left[\frac{W-1}{2}\left(\sigma + T\left(\prod_{j \neq i}\frac{1}{1 - \tau_j} - 1\right)\right) + T\prod_{j \neq i}\frac{1}{1 - \tau_j}\right]$$

$$= \frac{2\lambda_i}{P(W+1)}\left[\frac{W+1}{2}T\prod_{j \neq i}\frac{1}{1 - \tau_j} - \frac{W-1}{2}(T - \sigma)\right]$$

$$= \frac{\lambda_i T}{P} \prod_{j \neq i} \frac{1}{1 - \tau_j} - \frac{\lambda_i (W - 1)(T - \sigma)}{P(W + 1)}.$$

Using the first-order Taylor approximation, we have $\prod_{j \neq i} \frac{1}{1-\tau_j} \approx 1 + \sum_{j \neq i} \tau_j$. Hence,

$$\tau_i = \frac{\lambda_i T}{P}\Big(1 + \sum_{j \neq i} \tau_j\Big) - \frac{\lambda_i (W-1)(T-\sigma)}{P(W+1)},$$

which can be rewritten as

$$\tau_i = \Big(\frac{\lambda_i T}{P} \sum_j \tau_j + \frac{\lambda_i T}{P} - \frac{\lambda_i (W-1)(T-\sigma)}{P(W+1)}\Big)\Big/\Big(1 + \frac{\lambda_i T}{P}\Big).$$

Therefore, let $y = \sum_j \tau_j$, $\gamma_i^1 = \frac{\lambda_i T}{P}\big/\big(1 + \frac{\lambda_i T}{P}\big)$ and $\gamma_i^2 = \big(\frac{\lambda_i T}{P} - \frac{\lambda_i(W-1)(T-\sigma)}{P(W+1)}\big)\big/\big(1 + \frac{\lambda_i T}{P}\big)$, and we have

$$\tau_i = \gamma_i^1 y + \gamma_i^2.$$

Then, $\widetilde{\Sigma}$ is equivalent to

$$\widetilde{\Sigma}: \begin{cases} \tau_i = \gamma_i^1 y + \gamma_i^2 & (\text{a}') \\ y = \sum_i \big(\gamma_i^1 y + \gamma_i^2\big) & (\text{b}') \end{cases}$$

which admits only one solution, namely

$$\tau_i = \frac{\gamma_i^1 \sum_j \gamma_j^2}{1 - \sum_i \gamma_j^1} + \gamma_i^2.$$

APPENDIX E
MISCELLANEOUS

	$P_{idle;\{\cdot\}}$	$P_{succ;\{\cdot\}}$
$\mathbb{E}[slot_{i,\overline{Q}}]$	$\prod_{j \neq i}(1 - \tau_j)$	$\sum_{j \neq i} \tau_j \prod_{l \neq i,j}(1 - \tau_l)$
$\mathbb{E}[slot_{i,Q}]$	$(1 - \tau_{i,Q})\prod_{j \neq i}(1 - \tau_j)$ where $\tau_{i,Q} = \frac{1}{\overline{W}_i}$	$\sum_l t_l \prod_{j \neq l}(1 - t_l)$ where $t_j = \begin{cases} \tau_{i,Q}, & j = i \\ \tau_j, & j \neq i \end{cases}$
$\mathbb{E}[slot_{i,Q,\overline{Tx}}]$	$\prod_{j \neq i}(1 - \tau_j)$	$\sum_{j \neq i} \tau_j \prod_{l \neq i,j}(1 - \tau_l)$

TABLE I
SUMMARY OF COMPUTATION OF $\mathbb{E}[slot_{\{\cdot\}}]$.

Quant. with simplified comp.	Approx. and Assump.
$\overline{W}_i$	(i) successive attempts omitted; (ii) approximated by $\frac{W+1}{2}$ when W is large
$\overline{X}_i^p$	successive attempts omitted
$\mathbb{E}[slot_{\{\cdot\}}]$	(i) collisions involving three or more nodes omitted; (ii) $\overline{CW}_{\{\cdot\}}$ approximated by W
$\hat{\rho}$	numerically approximated by $\hat{\hat{\rho}}$
	FACS decoupling approximation or equivalently Bianchi's decoupling approximation when successive attempts omitted

TABLE II
SUMMARY OF SIMPLIFICATIONS MADE IN THE MODELING AND COMPUTATION.

Transmission rate per channel	5.5 Mbps
Data packet length P	1500 Bytes
DIFS	50 μs
SIFS	10 μs
ACK packet length (in time units)	203 μs
Header length (in time units)	192 μs
Empty system slot time σ	20 μs
Propagation delay δ	1 μs
Initial backoff window size W	32
Maximum backoff stage m	5
Data rate granularity $\Delta\lambda$	100 Kbps
Instability threshold constant	1%
Total simulated time T_f	10 seconds

TABLE III

SPECIFICATIONS OF THE IMPLEMENTATION OF TEST BENCH.

REFERENCES

[1] G. Bianchi, "Performance Analysis of the IEEE 802.11 Distributed Coordination Function," *IEEE Journal on Selected Areas in Communications*, vol. 18, pp. 535–547, 2000.

[2] A. Kumar, E. Altman, D. Miorandi, and M. Goyal, "New Insights from a Fixed Point Analysis of Single Cell IEEE 802.11 WLANs," *Proceedings of the IEEE INFOCOM 05*, vol. 3, pp. 1550 – 1561, 2005.

[3] K. Duffy, D. Malone, and D. J. Leith, "Modeling the 802.11 Distributed Coordination Function in Non-saturated Conditions," *IEEE Communications Letters*, vol. 9(8), pp. 715–717, 2005.

[4] G. R. Cantieni, Q. Ni, C. Barakat, and T. Turletti, "Performance Analysis under Finite Load and Improvements for Multirate 802.11," *Elsivier Computer Communications*, vol. 28(10), p. 10951109, 2005.

[5] D. Malone, K. Duffy, and D. J. Leith, "Modeling the 802.11 Distributed Coordination Function in Non-saturated Heterogeneous Conditions," *IEEE/ACM Transactions on Networking*, vol. 15(1), p. 159172, 2007.

[6] K. R. Duffy, "Mean Field Markov Models of Wireless Local Area Networks," *Markov Processes and Related Fields*, vol. 16(2), pp. 295–328, 2010.

[7] V. Anantharam, "The Stability Region of the Finite-User Slotted ALOHA Protocol," *IEEE Transactions on Information Theory*, vol. 37, pp. 535–540, 1991.

[8] A. Jindal and K. Psounis, "The Achievable Rate Region of 802.11-Scheduled Multi-hop Networks," *IEEE/ACM Transactions on Networking*, vol. 17(4), pp. 1118 – 1131, 2009.

[9] D. Leith, V. Subramanian, and K. Duffy, "Log-convexity of Rate Region in 802.11e WLANs," *IEEE Communications Letters*, vol. 14(1), pp. 57 – 59, 2010.

[10] J. D. C. Little, "A Proof for the Queuing Formula: $L = \lambda W$," *Operations Research*, vol. 9(3), pp. 383–387, 1961.

[11] G. Bianchi and I. Tinnirello, "Remarks on IEEE 802.11 DCF Performance Analysis," *IEEE Communications Letters*, vol. 9, pp. 765–767, 2005.

[12] Q. Wang and M. Liu, "Characterizing the Stability Region of IEEE 802.11 Distributed Coordination Function - Part II: A Multi-channel Perspective," tech. rep., 2011. http://www.eecs.umich.edu/~mingyan/pub.html.

[13] J. L. Massey and P. Mathys, "The Collision Channel Without Feedback," *IEEE Transactions on Information Theory*, vol. 31, pp. 192–204, 1985.